Dalton Transactions

RSC Publishing

PAPER

View Article Online
View Journal | View Issue

Cite this: *Dalton Trans.*, 2013, **42**, 11709

Copper(II) complex of methionine conjugated bis-pyrazole based ligand promotes dual pathway for DNA cleavage†

Sudipta Bhattacharyya,‡[a] Amrita Sarkar,‡[a] Suman Kr Dey,[a] Gregor P. Jose,[b] Arindam Mukherjee*[a] and Tapas K. Sengupta[b]

Received 12th April 2013,
Accepted 3rd June 2013

DOI: 10.1039/c3dt51296g

www.rsc.org/dalton

Three Cu^{II} complexes of bis-pyrazole based ligands have been synthesized and structurally characterized by X-ray crystallography. One of the ligand (**L2**) contains a methionine ester conjugated to a bis-pyrazole carboxylate through an amide linkage. The binding constant for complexes **1–3** with CT DNA are of the order of 10^4 M^{-1}. The crystal structure suggests that the axial Cu–O bonds (*ca.* 2.31(4) Å) are relatively labile and hence during the redox cycle with ascorbic acid and oxygen one or both the axial Cu–O bonds might open to promote copper oxygen reaction and generate ROS. The chemical nuclease activity of complexes **1–3** in dark, show complete relaxation of supercoiled DNA at 100 μM concentration in presence of ascorbic acid (H_2A). The mechanistic investigation suggests that the complexes **1** and **2** show involvement of peroxo species whereas **3** shows involvement of both singlet oxygen and peroxo species in DNA cleavage. The singlet oxygen formation in dark is otherwise unfavourable but the presence of methionine as pendant arm in **L2** might activate the generation of singlet oxygen from the metal generated peroxo species. The results of DNA cleavage studies suggest that methionine based copper(II) complexes can promote dual pathway for DNA cleavage. Probing the cytotoxic activity of these complexes on MCF-7, human breast cancer cell line shows that **3** is the most effective one with an IC_{50} of 70(2) μM.

Introduction

Ascorbic acid (H_2A) and glutathione (GSH) are two main extracellular and intracellular physiological reductants which may promote the redox process of metal ions. The cellular concentration of GSH is 1–10 mM and the extracellular concentration of H_2A is *ca.* 12–80 μM.[1] Higher concentration (1–10 mM) of ascorbate is found in intracellular compartments.[2,3] There are multiple reports which show that high dose of H_2A may be beneficial in cancer treatment either as standalone or in combination with other anti-cancer agents.[4] Ruthenium based anticancer agents like KP1019 is found to be more active with simultaneous high doses of H_2A.[5]

The chemical nuclease activity of Cu^{II} complexes is also known to be better in presence of external activators *viz.* H_2A, hydrogen peroxide (H_2O_2) and may proceed through different mechanistic pathways.[6] H_2A in combination with Cu^{II} is known to generate reactive oxygen species (ROS) that can kill cells, especially those which have lost the efficiency of anti-oxidative stress defence (*viz.* cancer cells).[7] The studies on mechanistic aspect of DNA cleavage by Cu^{II} complexes show involvement of various ROS ($^{\cdot}OH$, $O_2^{\cdot -}$, $^1O_2$, H_2O_2) depending on the ligand and the coordination number of the Cu^{II} ion.[6,8–27] It is thought that when peroxide mediated DNA cleavage is observed the reactive species might be a copper oxo species and the copper oxygen bond length plays an important role in superoxide mediated cleavage.[16–19] Cu^{II} complexes showing production of more than one ROS under same conditions may have potential for their capability of activating DNA damage through multiple pathways.[20–22,24]

A survey of the literature shows singlet oxygen based DNA cleavage in dark mediated by Cu^{II} complexes is rare.[20–23] Planar heterocyclic ligand based Cu^{II} complexes having methionine have shown photo-toxicity against SC DNA and various cancer cell lines mediated through generation of singlet oxygen or hydroxyl radical (Table S1†).[15,27–31] In addition Cu^{II} methionine complexes can cleave DNA in dark

[a]*Department of Chemical Sciences, Indian Institute of Science Education & Research Kolkata, Mohanpur Campus, P.O. BCKV Main Campus, Nadia, 741252, India. E-mail: a.mukherjee@iiserkol.ac.in; Fax: (+91)033-25873118; Tel: (+91)033-25873121*

[b]*Department of Biological Sciences, Indian Institute of Science Education & Research Kolkata, Mohanpur Campus, P.O. BCKV Main Campus, Nadia, 741252, India*

†Electronic supplementary information (ESI) available: Crystallographic data in CIF, cyclic voltammogram, UV/vis spectra of DNA binding, gel images of DNA cleavage by complexes. CCDC 916433–916435. For ESI and crystallographic data in CIF or other electronic format see DOI: 10.1039/c3dt51296g

‡Both the authors have equal contribution to this work.

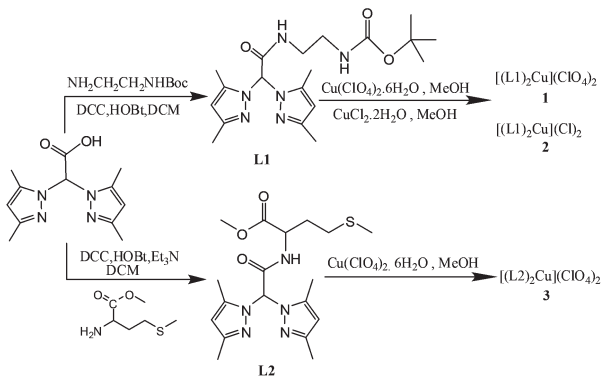

Scheme 1 General scheme for the synthesis of ligand **L1** and **L2** and metal complexes **1–3**.

selectively through hydroxyl radical[27] or singlet oxygen[23] (Table S1†). Generation of multiple ROS in a methionine based complex is scarce, the only known example is a V^{IV} complex which shows generation of $^{\cdot}OH$ and $^1O_2$ under same conditions in presence of light (Table S1†).[29] In addition studies suggest that presence of methionine has a positive effect in treating liver diseases[32,33] which is of importance in designing anticancer agents since they are known to cause liver stress.[34–38]

In our quest to study the effect of methionine when conjugated in a Cu^{II} complex herein we present the syntheses, structure, DNA cleavage and cytotoxicity studies of three Cu^{II} complexes of bispyrazolyl ligands (Scheme 1) to show that presence of methionine in copper complexes may also lead to activation of a dual pathway promoting peroxide and singlet oxygen based DNA cleavage in dark leading to better cytotoxicity. In order to probe the effect of methionine we have conjugated methionine as a pendant moiety selectively in one of the ligands (**L2**) and probed the relaxation of SC DNA using the Cu^{II} complexes $[Cu(L1)_2](ClO_4)_2$ (**1**), $[Cu(L1)_2](Cl)_2$ (**2**) and $[Cu(L2)_2](ClO_4)_2$ (**3**). The structures of the complexes have been solved using single crystal X-ray crystallography.

Experimental

Materials and physical measurements

All chemicals and solvents were purchased from commercial sources. Solvents were distilled and dried before use.[39] *N*,*N*′-Dicyclohexylcarbodiimide (DCC), 1-hydroxybenzotriazole (HOBt), ethidium bromide (EtBr), agarose (molecular biology grade) were purchased from SRL (India). Supercoiled pUC 19 DNA was purchased from Bangalore-Genei (India). Calf Thymus (CT) DNA and cisplatin was purchased from Sigma-Aldrich. All the solvents used for spectroscopy and lipophilicity measurements are of spectroscopy grade, purchased from Merck. The column chromatographic separations were performed using silica gel 60–120 mesh size (Merck-India). Melting point for the compounds were measured in triplicate with one end sealed capillaries using SECOR India melting point apparatus and the uncorrected values are reported. UV-Visible measurements were done using Varian Cary 300 Bio and Perkin Elmer lambda 35 spectrophotometer. FT-IR spectra were recorded using Perkin-Elmer SPECTRUM RX I spectrometer in KBr pellets. ^1H & proton decoupled ^{13}C NMR spectra were measured using either JEOL ECS 400 MHz or Bruker Avance III 500 MHz spectrometer at room temperature. The chemical shifts are reported in parts per million (ppm). Elemental analyses were performed on a Perkin-Elmer 2400 series II CHNS/O series. Electro-spray ionization mass spectra were recorded using micromass Q-Tof micro™ (Waters) by +ve mode electrospray ionization. The synthetic yields reported are of isolated analytically pure compounds. The ligands and complexes synthesized were dried in vacuum and stored in desiccator.

Caution! Perchlorate salts are explosive and corrosive so special care should be taken while handling those compounds.

Syntheses

Synthesis of bis(3,5-dimethyl pyrazole)carboxylic acid (bdmpza). The compound was synthesized using literature procedure.[40] Yield: 57%. ^1H NMR ($CDCl_3$, 400 MHz): δ 2.18 (s, 6H, CH_3), 2.23 (s, 6H, CH_3), 5.89 (s, 2H, H_{pz}), 6.80 (s, 1H, CH).

Synthesis of *tert*-butyl-*N*-(2-aminoethyl)carbonate. *tert*-butyl-*N*-(2-aminoethyl)carbonate was prepared by a reported method.[41] Yield: 80%. ^1H NMR ($CDCl_3$, 400 MHz) δ 1.43 (s, 9H, $3CH_3$), 2.78 (t, 2H, CH_2NH_2, J = 5.48 Hz), 3.15 (t, 2H, CH_2NH, J = 5.6 Hz), 4.90 (s, 1H, NH).

Synthesis of methyl-2-amino-4-(methylthio)butanoate. Methyl-2-amino-4-(methylthio)butanoate was prepared following previously reported procedure.[42] Yield: 98%. ^1H NMR ($CDCl_3$, 400 MHz) δ 2.01 (m, 2H, CH_2), 2.16 (s, 3H, CH_3), 2.40 (m, 2H, CH_2), 3.08 (s, 3H, $COOCH_3$), 4.38 (m, 1H, CH), 8.81 (s, 2H, NH_2).

Synthesis of *tert*-butyl-2-{2,2-bis(3,5-dimethyl-1*H*-pyrazolyl)}-acetamidethylcarbamate (L1). To a ice cold solution of bdmpza (6 g, 24 mmol) in dichloromethane *tert*-butyl-*N*-(2-aminoethyl)carbonate (7.73 g, 48 mmol) was added followed by the addition of DCC (4.94 g, 24 mmol) and HOBt (6.52 g, 48 mmol). The resulting mixture was stirred for 3 days. Upon completion (monitored by TLC) the reaction mixture was filtered to separate DCU. Then the resulting organic layer was washed with 2 N HCl (3 × 100 mL), brine (1 × 100 mL), 1 M sodium carbonate solution (2 × 100 mL) and then brine solution (2 × 50 mL) respectively. The resulting organic layer was dried over anhydrous Na_2SO_4 and evaporated under vacuum. The crude product thus obtained was further purified by column chromatography on silica gel with ethyl acetate–hexane (7 : 3) mixture to give compound **L1** as a white microcrystalline mass. Yield: 6.89 g (73%). Mp: 138 °C. Anal. Calc. for $C_{19}H_{30}N_6O_3$: C, 58.44; H, 7.74; N, 21.52%. Found: C, 58.39; H, 7.78; N, 21.49%. UV-vis λ_{max}/nm (ε/dm^3 mol^{-1} cm^{-1}) in CH_3OH: 227 (9200), 280 (23). IR (KBr) (ν_{max}/cm^{-1}) 3337s, 3060w, 2965s, 2980s, 2950s, 2930s; 1716w, 1688s, 1676s, 1562s, 1537s, 1444m, 1417s, 1370s, 1337s, 1287s, 1273s, 1254s, 1177s, 1135w, 1030s, 974w, 985w, 939w, 842m, 820w, 728w, 710w, 670w, 483w. ^1H NMR ($CDCl_3$, 500 MHz) δ 1.42

(s, 9H, $3CH_3$ of BOC), 2.21 (s, 6H, CH_3), 2.25 (s, 6H, CH_3), 3.37 (t, J = 5.0 Hz, –$NHCH_2$), 3.40 (t, J = 6.0 Hz, $NHCH_2CH_2$), 5.84 (s, 2H, H_{pz}), 6.58 (s, 1H, CH), 7.75 (s, 1H, CONH). ^{13}C NMR ($CDCl_3$ 125 MHz): δ 11.06 (CH_3), 13.64 (CH_3), 28.37 (t-CH_3), 39.41 (CH_2), 40.13 (CH_2), 70.72 (CH), 79.12 (t-C), 107.12 (CH), 140.67 (C_{pz}), 149.68 (C_{pz}), 156.26 (CO), 164.95 (CO). ESI-MS (CH_3OH), m/z (calc.): 413.22 (413.23) $[M + Na]^+$.

Synthesis of methyl 2-(2,2-bis(3,5-dimethyl-1*H*-pyrazole-1-yl)-acetamido)-4-(methylthio)butanoate (L2). Bdmpza (0.49 g, 2 mmol) was dissolved in dry DCM at 0 °C. The methyl-2-amino-4-(methylthio)butanoate (0.79 g, 4 mmol) and Et_3N (0.45 g, 0.612 mmol) were added to the ice cooled solution. Finally DCC (0.42 g, 2 mmol) and HOBt (0.54 g, 4 mmol) were added to the above reaction mixture. The reaction was stirred for 3 days and monitored by TLC. The precipitated DCU was filtered off and the organic layer was washed sequentially with HCl (2 N, 3 × 20 mL), brine (1 × 20 mL), sodium carbonate (2 N, 3 × 20 mL) and brine (2 × 20 mL). The organic layer was dried over anhydrous Na_2SO_4 and evaporated under vacuum. The pale yellow solid obtained was purified by column chromatography on silica gel with ethyl acetate–hexane (7 : 3) mixture to give the ligand **L2** as white solid. Yield: 0.50 g (63%). Mp: 86 °C. Anal. Calc. for $C_{18}H_{27}N_5O_3S$: C, 54.94; H, 6.92; N, 17.80; S, 8.15%. Found C, 54.85; H, 6.95; N, 17.72; S, 8.10%. UV-vis λ_{max}/nm (ε/dm^3 mol^{-1} cm^{-1}) in CH_3CN: 194 (17 700), 223 (10 020), 318 (30). IR (KBr) (ν_{max}/cm^{-1}) 3303s, 3075w, 2992w, 2946s, 2925s, 2375w, 1736s, 1702s, 1628w, 1553s, 1438s, 1389m, 1306w, 1279m, 1248m, 1164m, 1115w, 1013s, 974m, 887m, 784s, 642m, 622m, 532m, 418m. ^{1}H NMR ($CDCl_3$, 400 MHz) δ 2.06 (s, 3H, SCH_3), 2.18 (s, 3H, CH_3), 2.19 (s, 3H, CH_3), 2.29 (s, 3H, CH_3), 2.33 (s, 3H, CH_3), 2.62 (t, J = 7.36 Hz, 2H, CH_2SCH_3), 3.45 (s, 2H, CH_2), 3.73 (s, 3H, CH_3), 4.76 (m, 1H, CH_2COOCH_3), 5.85 (d, J = 4.28 Hz, 2H, CH_{pz}), 6.70 (s, 1H, CH), 8.26 (d, J = 7.96 Hz, 1H, NH). ^{13}C NMR ($CDCl_3$ 125 MHz) δ 11.16 (CH_3) 11.22 (CH_3), 15.30 (SCH_3), 29.65 ($CH_2CH_2SCH_3$), 31.32 ($CH_2CH_2SCH_3$), 52.04 ($NHCH_2$), 71.13 (OCH_3), 52.42 (CHNN), 107.15 (Ar-C), 140.80 (Ar-C), 141.56 (Ar-C), 149.14 (Ar-C), 149.56 (Ar-C), 164.20 (CO_{amide}), 171.515 (CO_{ester}). ESI-MS (CH_3OH), m/z (calc.): 394.02 (394.19) $[M + H]^+$.

Synthesis of $[Cu(L1)_2](ClO_4)_2$ (1). The ligand **L1** (2 g, 5.12 mmol) was dissolved in 35 mL of dry methanol and the solution degassed by purging N_2. Solid $Cu(ClO_4)_2{\cdot}6H_2O$ (0.943 g, 2.55 mmol) was added in instalment to this solution for 5 min. Then the solution was stirred for 6 h under N_2. A light blue coloured mass precipitated out from the mixture which was filtered by suction and vacuum dried. The isolated compound was recrystallized from acetonitrile to give the pure complex **1**. Yield: 76%. Mp: 217 °C (decomp.). Anal. Calc. for $C_{38}H_{60}Cl_2N_{12}O_{14}Cu$: C, 43.74; H, 5.80; N, 16.11%. Found: C, 43.67; H, 5.85; N, 16.17%. UV-vis λ_{max}/nm (ε/dm^3 mol^{-1} cm^{-1}) in CH_3CN: 223 (39 100), 273 (780), 322 (740), 631 (8). IR (KBr) (ν_{max}/cm^{-1}) 3644s, 3487br, 3417m, 3301m, 3104s, 3009w, 2974s, 2934br, 2043w, 1696s, 1675s, 1632w; 1564s, 1513m, 1463m, 1445m, 1422w, 1394m, 1348w, 1311m, 1272m, 1257m, 1242m, 1166m, 1117s, 1052s, 955w, 993m, 929w, 876w, 830w, 773w, 756w, 651w, 624w, 488w. ESI-MS (CH_3CN), m/z (calc.): 842.46 (842.40) $[M - H]^+$, 421.68 (421.70) $[M]^{2+}$.

Synthesis of $[Cu(L1)_2](Cl)_2$ (2). To a degassed methanolic solution of **L1** (1.5 g, 3.84 mmol) an aqueous methanolic solution of $CuCl_2{\cdot}2H_2O$ (0.327 g, 1.92 mmol) was added at once with constant stirring. The whole solution was stirred at room temperature for 6 h. The resulting green colour solution was filtered and the filtrate kept for slow evaporation. After one week the deep blue coloured crystals of compound **2** separated which were washed with minimum volume of ether and dried under vacuum. Yield: 0.8 g (45%). Mp: 220 °C (decomp.). Anal. Calc. for $C_{38}H_{60}N_{12}Cl_2O_6Cu$: C, 49.86; H, 6.61; N, 18.36%. Found: C, 49.93; H, 6.67; N, 18.40%. UV-vis λ_{max}/nm (ε/dm^3 mol^{-1} cm^{-1}) in CH_3OH: 215 (39 300), 273 (860), 317 (800), 645 (7). IR (KBr) (ν_{max}/cm^{-1}) 3562s, 3442s, 3405m, 3280m, 3180w, 3135w, 3071m, 2980m, 2933m, 2848w, 2799m, 2059w, 1697s, 1673s, 1584m, 1561m, 1516m, 1464m, 1420m, 1400w, 1362m, 1353m, 1313m, 1275m, 1247m, 1163m, 1148m, 1117s, 1098m, 1052w, 994w, 973w, 957w, 777w, 755w, 636w, 487m. ESI-MS (CH_3OH) m/z (calc.): 842.41 (842.40) $[M - H]^+$, 421.73 (421.70) $[M - H]^{2+}$.

Synthesis of $[Cu(L2)_2](ClO_4)_2$ (3). A 4 mL methanolic solution of $Cu(ClO_4)_2{\cdot}6H_2O$ (0.093 g, 0.25 mmol) was added to a 10 mL solution of **L2** (0.19 mg, 0.50 mmol) in methanol under stirring condition. After few minutes a light blue coloured precipitation started to appear. Stirring was continued for additional 3 hours to complete the reaction. The resultant solution was filtered and the precipitate washed with methanol and re-dissolved in dichloromethane. The dichloromethane solution was layered with hexane to obtain **3** as blue crystals. Yield: 0.17 g (64%). Mp: 234 °C (decomp.). Anal. Calc. for $C_{36}H_{54}Cl_2N_{10}O_{14}S_2Cu$: C, 41.20; H, 5.19; N, 13.35%; S, 6.11%. Found: C, 41.55; H, 5.23; N, 13.31%; S, 6.05%. UV-vis λ_{max}/nm (ε/dm^3 mol^{-1} cm^{-1}) in CH_3CN: 206 (46 000), 223 (36 550), 325 (715), 624 (15). IR (KBr) (ν_{max}/cm^{-1}): 3644s, 3487br, 3417m, 3301m, 2043w, 1696s, 1675s, 1632w; 1564s, 1513m, 1463m, 1445m, 1422w, 1394m, 1348m. ESI-MS (CH_3CN), m/z (calc.): 424.15 (424.14) $[M]^{2+}$.

X-ray crystal structure determination

Good quality single crystals suitable for X-ray diffraction were obtained from the slow evaporation of acetonitrile solution of **1** and **2**. Single crystals of **3** were obtained by layering a dichloromethane solution with hexane. The single crystals of **1–3** were mounted using loops on the goniometer head of a Bruker Kappa Apex II CCD Duo diffractometer with graphite monochromated Mo-Kα radiation (0.71073 Å) and data collected at a temperature of 100 K. An empirical multi-scan absorption correction was performed using SADABS.[43] The structures were solved by direct methods and all non-hydrogen atoms were refined anisotropically by full matrix least-squares on F^2. The hydrogen atoms were calculated and fixed using SHELXL-97 after hybridization of all non hydrogen atoms.[44] Few residual electron densities which appeared to be disordered lattice solvent molecules could not be modeled properly and were showing high motion during refinements hence

we have used SQUEEZE provision in PLATON which lead to a fully converged well refined structure.[45] The crystallographic data for the structures have been deposited at the Cambridge Crystallographic Data Centre as supplementary publication CCDC 916433 (**1**), 916434 (**2**) and 916435 (**3**).†

Electrochemistry

Electrochemical studies were carried out with a Princeton Applied Research 263A potentiostat and galvanostat using a platinum (Pt) disc working, a platinum wire counter and a non-aqueous Ag/Ag^{+} reference electrode (0.55 V w.r.t. NHE, quantified using the ferrocene Fe^{2+}/Fe^{3+} couple). The voltammograms were recorded using 0.1 M TBAP as supporting electrolyte in DMF solvent. The copper complexes **1–3** and their corresponding free ligands were used in 1 mM concentration during measurements. All the experimental data discussed were done at a scan rate of 50 mV s^{-1}.

DNA interaction studies

Preparation of stock DNA solution. A concentrated stock solution of CT DNA was prepared in 50 mM Tris–HCl/50 mM NaCl in water at pH 7.4. The concentration of CT DNA was determined by measuring absorbance at 260 nm using the ε_{260} of DNA as 6600 dm^3 mol^{-1} cm^{-1}.[46] The CT DNA was found to be sufficiently free of protein since the UV absorbance ratio at 260 and 280 nm was found to be *ca.* ~1.9.[47] The stock DNA solution was stored at 4 °C and used within four days.

Binding studies with CT DNA. Interaction of the Cu^{II} complexes **1**, **2** and **3** with CT DNA were measured with the help of UV-vis spectroscopy in tris buffer–DMF (9 : 1) media (v/v). The same medium was also used for preparation of stock solution of complexes. Spectroscopic titrations were carried out at room temperature. The concentration of the complexes **1–3** for the binding experiments was fixed to 4×10^{-4} M. The change in the absorbance was monitored with subsequent addition of an aliquot of 6 μL (concentration of 4×10^{-3} M) CT DNA in the sample and reference cuvette. The spectra were recorded after equilibration of the mixture for 10 min after each addition. The titration was continued until there was no significant change in absorbance for at least five successive additions.

Thermal denaturation. The thermal denaturation of CT DNA was performed with complexes **1–3** on Varian Cary 300 Bio equipped with a thermostatic cell holder. CT DNA (60 μM) was treated with **1–3** in a 1.5 : 1 ratio (DNA : complex) in buffer (50 mM Tris–HCl/50 mM NaCl, pH 7.4)–DMF mixture of 9 : 1 (v/v). The samples were heated from 30–90 °C at a rate of 1 °C min^{-1} with a hold time of 30 s between each increment and the change in absorption at 260 nm was monitored. The melting temperatures (T_m) for the CT DNA alone or upon binding with complexes were determined as when half of the ds DNA become ss DNA (Fig. 5).

DNA cleavage studies. The oxidative cleavage of supercoiled pUC19 DNA (2 μL, *ca.* 300 ng) was performed with different concentrations of **1** and **3**. Two separate set of experiments were carried out in presence of varying concentrations of hydrogen peroxide (to exploit the $Cu^{II/III}$ redox couple) and ascorbic acid (to exploit the $Cu^{I/II}$ redox couple). The incubation period was 1.5 h at 37 °C for all DNA cleavage experiments reported.[48,49] Stock solutions of the three complexes were made in DMF. The DNA cleavage experiments for all the complexes were carried out in a 9 : 1 v/v ratio of 50 mM Tris–HCl buffer and DMF having 50 mM NaCl and a pH of 7.4. Photocleavage experiments were carried out at 365 nm using a 4 W UV light (Spectroline®). The samples were irradiated for 30 min followed by an 1 h incubation in dark at 37 °C. After completion of incubation the samples were ice cooled for 15 min and a bromophenol blue based loading dye (3 μL) was added to the samples. The samples were then loaded on a 1% (w/v) agarose gel containing 1.0 μg mL^{-1} EtBr in 1× TAE (Tris–acetic acid–EDTA) buffer. Electrophoresis was performed at 50 V for 4 h in 1× TAE buffer. The bands were visualised using gel documentation system (Bio-Rad) and quantifications were done using Image Lab v4.0.1 software. In all the cases the background fluorescence was subtracted. The emission intensities of the SC plasmid bands were corrected by a factor of 1.3[50,51] since the ability of EtBr to intercalate into supercoiled (SC) DNA is less compared to the nicked-circular (NC) form. The time dependent DNA cleavage studies for **1–3** (100 μM) were done same as above except that the samples were incubated for variable time (0–60 min) in presence of 5 molar equivalent of H_2A and reaction mixture was quenched by addition of loading dye followed by keeping at −30 °C.

Lipophilicity measurement

Partition coefficient of the complexes in octanol–water system was determined using standard shake-flask method.[52] Octanol and water (equal volume) were pre-equilibrated overnight before the experiment.[53] After equilibration the solid samples were added to the mixture of solvents and shaken on a dancing shaker overnight at room temperature. On the next day the tubes were centrifuged and left undisturbed for an hour. Aliquots of the aqueous and octanol layers were pipetted out separately and the absorbance measured using UV-vis spectroscopy. Concentration of the substances in each layer was calculated using the respective molar extinction coefficients of **1–3**.

Cytotoxicity assay

Human breast adenocarcinoma cell line (MCF-7) was maintained in the logarithmic phase at 37 °C in a 5% carbon dioxide atmosphere using a culture media containing DMEM, 10% foetal bovine serum (GIBCO), antibiotics (100 units mL^{-1} penicillin and 100 mg mL^{-1} streptomycin).

The cytotoxic effect of complexes **1–3** on MCF-7 cells was evaluated by means of MTT (tetrazolium salt reduction) assay.[54] Briefly, 6×10^3 cells per well, were seeded in 96-well plates in growth medium (200 μL) and then incubated at 37 °C in a 5% carbon dioxide atmosphere. After 48 h, the medium was removed and replaced with a fresh one and compounds to be studied were added at appropriate

concentrations. Triplicates for each concentration were used in the wells. The compounds to be added were solubilised in media or PBS containing DMSO (when needed) such that the concentration of DMSO in well should not exceed 0.2%. Cisplatin was dissolved in DMSO just before the experiment and a calculated amount of drug solution was added to the growth medium containing cells such that the final DMSO concentration in the wells were no more than 0.2%. After 48 h the media containing compound was removed and fresh media was added to each well and successively treated with 20 μL of a 2 mg mL^{-1} MTT in saline solution, followed by 3 h of incubation at 37 °C in 5% carbon dioxide atmosphere. After 3 h media was removed and 100 μL of DMSO (molecular biology grade) added to each well. The inhibition of cell growth induced by the tested complexes was detected by measuring the absorbance of each well at 515 nm[55,56] using a BIOTEK ELx800 plate reader. All experiments had the respective controls and standards as needed. IC_{50} values represent the drug concentration that reduces the mean absorbance at 515 nm to 50% as compared to the untreated control wells.

Results

X-Ray data and crystal structures

The complexes **1–3** have been synthesized and structurally characterised by single crystal X-ray crystallography. The ligands **L1** and **L2** only differ in the attached pendant group. The pendant group in **L1** is a BOC-protected ethylenediamine and in **L2** it is a methyl ester of methionine. Crystallographic data and refinement parameters for the three complexes **1–3** are summarised in Table S2.† The selected bond distance and angles are summarised in Table 1. **1** and **2** are complexes of **L1** and differ in terms of the anions (**1** has perchlorate and **2** has chloride). Complex **1** crystallizes in monoclinic space group *C*2/*c* whereas the chloride anion bearing complex **2** crystallizes in triclinic space group $P\bar{1}$ (Fig. 1 & S1† respectively). Complex **3** having the pendant methionine bearing **L2** as the ligand crystallizes in space group *P*1 (Fig. 2). The structural data show that in all the complexes the metal has N_4O_2 coordination. Bond valence sum (BVS) calculations[57] show that the central metal atoms are dipositively charged (Table S3†). Complexes **1–3** show distorted octahedral coordination at the Cu^{II} centers. All the complexes are dipositively charged and have a N_4O_2 coordination where the N-donors, situated in the square plane are the pyrazole nitrogen and the axially co-ordinated oxygens belong to the carbonyl group of the amide in **L1** and **L2**. The average Cu–N distance in **1–3** is 2.02(3) Å and the average Cu–O distance for the axial Cu–O bonds is *ca.* 2.31 (4) Å.

Electrochemistry

Cyclic voltammetry (CV) experiments of **L1**, **L2** and complexes **1–3** showed multiple reduction and oxidation peaks attributed to the ligands and the metal ions. The ligand **L1** showed a redox couple in the cathodic scan with an $E_{1/2}$ (ΔE_p) value of −1.3 V (60 mV) (Fig. S2†). However the ratios of the peak height current (i_{pa}/i_{pc}) were poor. The redox event for **L2** showed an $E_{1/2}$ (ΔE_p) of −1.27 V (140 mV) (Fig. S2†). Both the ligands also show an irreversible oxidation peak at *ca.* 0.39 V (0.37 V for **L1** and 0.41 V for **L2**). In the complexes **1–3** a reduction peak appears in the range of −0.67 to −0.78 V with a corresponding oxidation peak in the range −0.49 to −0.58 V (Fig. 3). Complex **2** shows an additional redox couple with $E_{1/2}$ = −0.097 V (ΔE_p = 193 mV). Complex **3** show an irreversible

Table 1 Selected bond lengths (Å) and angles (°) for complexes **1–3**

	1	**2**
Cu(1)–N(1)	2.03(1)	2.04(1)
Cu(1)–N(3)	2.02(3)	2.03(2)
Cu(1)–O(1)	2.32(2)	2.29(1)
N(1)–Cu(1)–O(1)	85.30(6)	84.59(6)
N(3)–Cu(1)–O(1)	84.11(6)	85.41(6)
N(3)–Cu(1)–N(1)	86.61(7)	86.79(7)
N(3A)[a]–Cu(1)–N(1)	93.39(7)	93.21(7)
N(1)–Cu(1)–O(1A)[a]	94.70(6)	95.41(6)
N(3)–Cu(1)–O(1A)[a]	95.96(9)	94.59(6)
N(3A)[a]–Cu(1)–N(3)	180.00(1)	180.00(1)
O(1)1–Cu(1)–O(1A)[a]	180.00(1)	180.00(7)

3			
Cu(1)–N(1)	2.01(7)	N(3)–Cu(1)–N(6)	179.3(2)
Cu(1)–N(3)	2.03(5)	N(1)–Cu(1)–O(1)	85.51(16)
Cu(1)–N(6)	2.04(1)	N(3)–Cu(1)–O(1)	82.92(14)
Cu(1)–N(8)	2.01(1)	N(6)–Cu(1)–O(1)	97.77(13)
Cu(1)–O(1)	2.33(1)	N(8)–Cu(1)–O(1)	96.43(15)
Cu(1)–O(2)	2.34(0)	N(1)–Cu(1)–O(2)	94.24(14)
N(1)–Cu(1)–N(3)	87.10(2)	N(3)–Cu(1)–O(2)	94.34(13)
N(1)–Cu(1)–N(6)	93.8(2)	N(6)–Cu(1)–O(2)	84.98(13)
N(1)–Cu(1)–N(8)	178.6(2)	N(8)–Cu(1)–O(2)	84.90(14)
N(8)–Cu(1)–N(3)	93.8(2)	O(2)–Cu(1)–O(1)	177.03(14)
N(8)–Cu(1)–N(6)	85.3(2)		

[a] A = $-x+2, -y+1, -z+1$ for **1** and $-x, -y+1, -z+1$ for **2**.

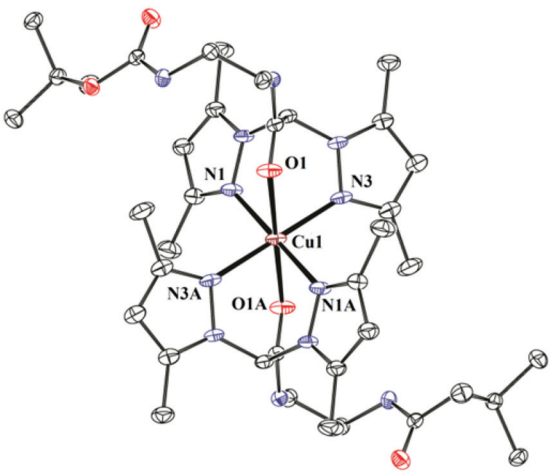

Fig. 1 ORTEP diagram of **1**. Thermal ellipsoids are drawn at 50% probability level. Hydrogen atoms, counter anions and solvents have been omitted for clarity. Symmetry transformations used to generate equivalent atoms A: $-x+2$, $-y+1$, $-z+1$.

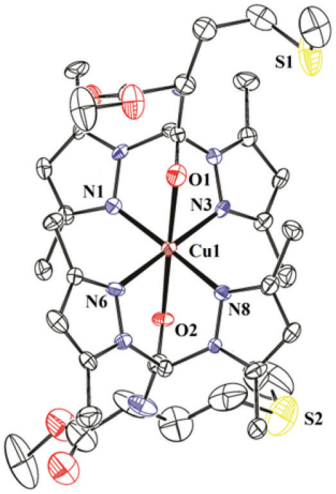

Fig. 2 ORTEP diagram of **3**. Thermal ellipsoids are drawn at 50% probability level. Hydrogen atoms, counter anions and solvents have been omitted for clarity.

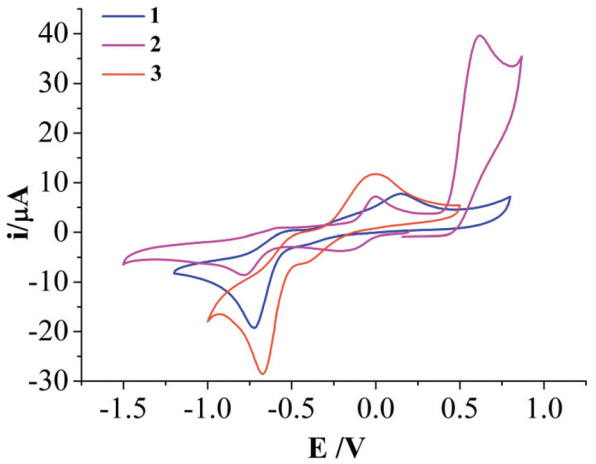

Fig. 3 Cyclic voltammogram of complexes **1–3** at 50 mV s^{-1} scan rate in DMF medium using non-aqueous 0.01 M Ag/Ag^{+} reference electrode (0.55 V w.r.t. NHE) showing the irreversibility of the $Cu^{II/I}$ redox couple.

redox couple with a reduction at −0.41 V and oxidation at −0.01 V. However, for all the redox event the oxidation peak height is much less than the reduction peak height. Complex **2** also shows an irreversible oxidation at 0.61 V which is not exhibited by **1** or **3**.

CT-DNA binding studies

Addition of DNA to the solution of **1–3** led to decrease in absorbance at around 247, 276 and 335 nm (Fig. S3†). The change in absorbance of the complex at 247 nm, upon formation of DNA–complex conjugate, with increasing concentration of DNA was used for the binding studies. The addition ratio (R) for the complexes was upto 1.5, where R = [DNA]/[Complex]. The change in the concentration of the metal complex and DNA due to dilution was duly corrected. The binding constants (K_b) for the complexes were determined

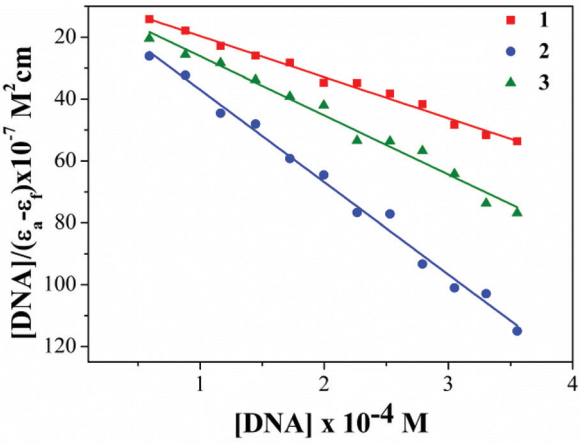

Fig. 4 Plot of $[DNA]/(\varepsilon_a - \varepsilon_f)$ *vs.* [DNA] for the determination of the apparent binding constant (K_b) of **1–3**.

Table 2 CT DNA binding parameters for complexes **1–3**. The estimated standard deviation for the binding constants from three trials are given in parentheses. The ΔT_m values vary within ±0.5 °C

Complex	$\Delta\varepsilon^a$	Hypochromism (%)	$\Delta\lambda$	K_b (M^{-1})	ΔT_m (°C)
1	1759	74	6	$2.0(2) \times 10^4$	1
2	1706	72	5	$4.9(5) \times 10^4$	2
3	2647	86	6	$3.1(3) \times 10^4$	1

[a] Units in $dm^3\ mol^{-1}\ cm^{-1}$.

from the spectroscopic titration data using the following equation.[58]

$$[DNA]/|(\varepsilon_a - \varepsilon_f)| = [DNA]/|(\varepsilon_b - \varepsilon_f)| + 1/K_b|(\varepsilon_b - \varepsilon_f)|$$

where [DNA] is the concentration of CT-DNA, $\varepsilon_a = A_{obsd}/[compound]$, ε_f = the extinction coefficient for the free (unbound) compound and ε_b = the extinction coefficient for the compound in the fully bound form. A plot of $[DNA]/(\varepsilon_a - \varepsilon_f)$ *vs.* [DNA] gives a slope $[1/(\varepsilon_b - \varepsilon_f)]$ and an intercept $[1/K_b\ (\varepsilon_b - \varepsilon_f)]$ and K_b is calculated from the ratio of slope and intercept. Complexes **1–3** showed hypochromism and bathochromic shift ($\Delta\lambda$) (Fig. 4, Fig. S3†). The binding constants obtained are of the order of $10^4\ M^{-1}$ (Table 2).

Thermal denaturation of CT-DNA

The thermal denaturation studies were performed with CT-DNA in the absence and presence of Cu^{II} complexes to determine the nature of binding. The hyperchromicity of CT DNA with increasing temperature in presence and absence of **1–3** was measured. The T_m value obtained for **1–3** is the temperature where half of the DNA unwinds. This transition point was calculated from mid-point of the melting curve (Fig. 5). There was an increase in the melting temperature (T_m) of 1 °C for **1** and **3** and 2 °C for **2** (Table 2).

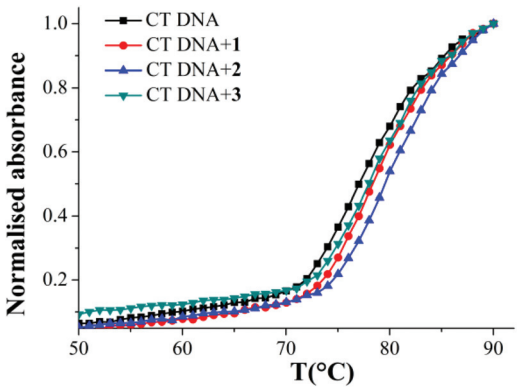

Fig. 5 CT DNA melting curve for free DNA and in presence of complexes **1–3** showing that binding is stronger for **2**. The legends on the top left show the colour scheme.

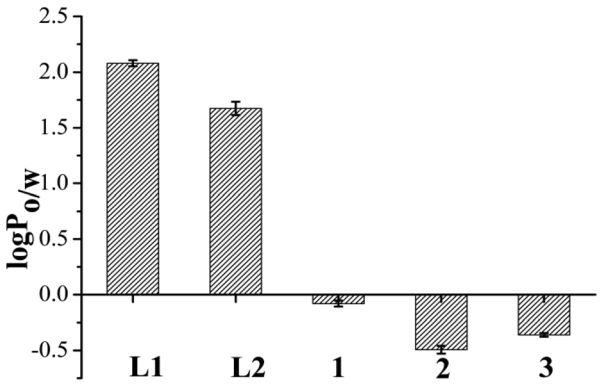

Fig. 6 Lipophilicity of the ligands and complexes **1–3** represented by a bar diagram showing comparative log *P* values of **L1**, **L2** and **1–3** in octanol–water system, where error bars in the graph represent the standard deviation in measurement.

Lipophilicity measurement

The partition coefficients to determine the lipophilicity of the ligands (**L1** and **L2**) and complexes (**1–3**) were calculated using the well known formula of log $P = C_{oct}/C_{aq}$ where C_{oct} was the concentration of complex in organic layer and C_{aq} was the concentration of complex in water found through UV-visible spectroscopy. The results displayed in Fig. 6 and Table S4† show that the lipophilicity or the log $P_{o/w}$ for the **L2** is less than **L1**. The complexes **1–3** were probed for their lipophilicity and found that the chloride anion bearing complex **2** is the most hydrophilic among the three complexes and lipophilicity order is **1** > **3** > **2**.

DNA cleavage

The three Cu^{II} complexes **1**, **2** and **3** in absence of any redox agent do not show any significant cleavage even at 170 μM concentration (Fig. S4†). However, in presence of 700 μM H_2O_2 at a concentration of 170 μM *ca.* 40% of NC form was generated by **1** and **2** and *ca.* 72% by **3** (Fig. S4†). Incubation of 80–100 μM complexes **1–3** with pUC19 SC DNA for 1.5 h in

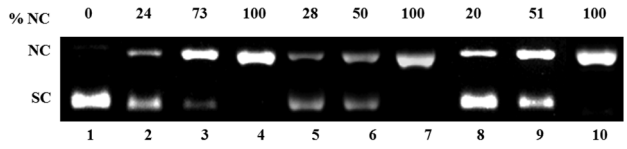

Fig. 7 Oxidative DNA cleavage of pUC 19 DNA (300 ng) in presence of 5 eq. ascorbic acid (H_2A) by various concentrations of complexes **1–3** in 50 mM Tris–HCl/NaCl buffer (pH = 7.4) after 1.5 h incubation at 37 °C. Lane 1, DNA control; lane 2–4, DNA + **1** (80, 90 and 100 μM respectively); lane 5–7, DNA + **2** (80, 90 and 100 μM respectively); lane 8–10, DNA + **3** (80, 90 and 100 μM) respectively.

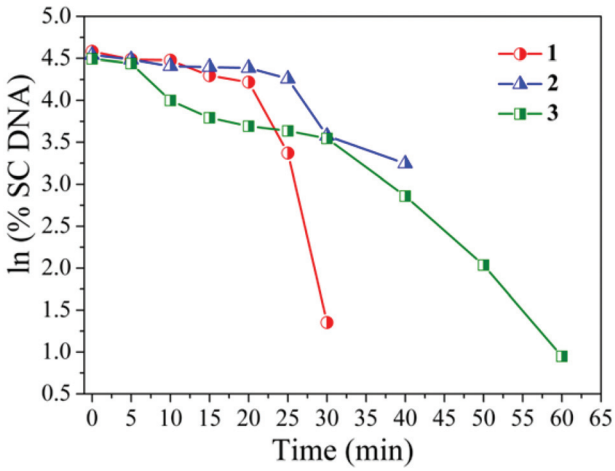

Fig. 8 Time dependent conversion of pUC19 SC DNA to its NC form by complexes **1–3** in presence of [DNA] = 300 ng, [Complex] = 100 μM and [H_2A] = 500 μM. A plot of ln (%SC DNA) *vs.* time for complex **1–3** showing a sudden decrease in the SC form beyond 20 min for **1**.

presence of 5 molar equivalent H_2A exhibited upto 100% relaxation of SC DNA to the NC form (Fig. 7).

Complexes **1–3** were probed for time dependent oxidative cleavage activity.[14,59] We found that there is a sudden increase in formation of NC DNA after around 20–30 min incubation period with all the complexes (Fig. 8, Fig. S5†) and after 30–60 min of incubation with 100 μM of **1–3**, and 500 μM H_2A as reducing agent, complete relaxation of the SC DNA is observed. The initial relaxation rate of complex **3** is faster as compared to **1** and **2**.

Next the ROS species involved in DNA damage was investigated using known ROS scavengers *viz.* DMSO, NaN_3, histidine, catalase and TEMPO. The control experiment with H_2A (500 μM) but no complex showed *ca.* 15% conversion to NC form suggesting that H_2A may itself be involved in ROS generation. 100 μM of complex **1** showed around *ca.* 90% of the NC form along with some linearized form and this remained unchanged in presence of DMSO, NaN_3 and histidine (Fig. 9). However, in presence of catalase and TEMPO the DNA cleavage activity of complex **1** and **2** decreased to 1/3 of its original value (Fig. 9 & S6† respectively). In case of complex **3** also DMSO did not decrease the DNA cleavage activity. However, the presence of singlet oxygen scavengers NaN_3 and especially histidine markedly decrease the generation of NC form

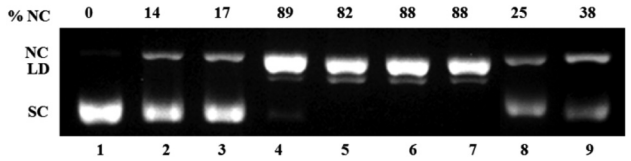

Fig. 9 Mechanistic study for oxidative DNA cleavage of pUC 19 DNA (300 ng) in presence of 5 eq. ascorbic acid (H_2A) by complex **1** (100 μM) in 50 mM Tris–HCl/NaCl buffer (pH = 7.4) after 1.5 h incubation at 37 °C using DMSO (1 eq.), NaN_3 (1 eq.), histidine (1 eq.), catalase (10 U) and 4-carboxy TEMPO (1 eq.). Lane 1, DNA control; lane 2, DNA + DMSO; lane 3, DNA + NaN_3; lane 4, DNA + **1**; lane 5, DNA + **1** + DMSO; lane 6, DNA + **1** + NaN_3; lane 7, DNA + **1** + histidine; lane 8, DNA + **1** + catalase; lane 9, DNA + **1** + 4-carboxy TEMPO.

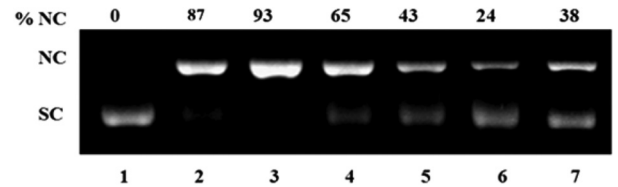

Fig. 10 Mechanistic study for oxidative DNA cleavage of pUC 19 DNA (300 ng) in presence of 5 eq. ascorbic acid (H_2A) by complex **3** (100 μM) in 50 mM Tris–HCl/NaCl buffer (pH = 7.4) after 1.5 h incubation at 37 °C using DMSO (1 eq.), NaN_3 (1 eq.), histidine (1 eq.), catalase (10 U) and 4-carboxy TEMPO (1 eq.). Lane 1, DNA control; lane 2, DNA + **3**; lane 3, DNA + **3** + DMSO; lane 4, DNA + **3** + NaN_3; lane 5, DNA + **3** + histidine; lane 6, DNA + **3** + catalase; lane 7, DNA + **3** + 4-carboxy TEMPO.

(Fig. 10). There was loss of activity in presence of catalase, the peroxide mediated DNA cleavage inhibitor.

To probe if singlet oxygen generation is enhanced in presence of light instead of a reducing agent, the complexes and DNA were exposed to a 4 W 365 nm UV light for 30 min followed by 1 h incubation in dark. However, even in presence of 170 μM of **1–3** only upto *ca.* 6% NC form was observed (Fig. S7†).

Cell cytotoxicity

MCF-7 cells were treated with the ligands **L1**, **L2** and complexes **1–3** to probe the *in vitro* cytotoxicity. The well known compound cisplatin was used as a standard in each 96 well plate. The results obtained show that **L1** and **L2** has IC_{50} value above 250 μM. Between **1** and **2**, **2** having the chloride counter anion is more effective (IC_{50} = 116(3) μM) than **1** (IC_{50} = 160(5) μM) bearing the perchlorate as counter anion. However, complex **3** is the most effective with an IC_{50} of 70(2) μM. The obtained data are plotted and fitted using GraphPad Prism® Ver 5.03 (Fig. S8†). IC_{50} values are summarised in Table 3.

Discussion

The ligands **L1** and **L2** show strong IR bands at 1676 and 1703 cm^{-1} respectively corresponding to $\nu_{C=O}$ of the amide. In addition **L2** has a strong IR band at 1736 cm^{-1} corresponding to the $\nu_{C=O}$ of the methyl ester of the conjugated methionine. **L1** has a strong IR band at 1688 cm^{-1} corresponding to the $\nu_{C=O}$ of the BOC conjugated amine. In complex **1–3** the $\nu_{C=O}$ of the amide appears at 1675, 1673 and 1675 cm^{-1} respectively suggesting weak bonding of the –C=O oxygen to the metal center. The ligands show a strong peak in the region of 1550–1562 cm^{-1} attributed to the $\nu_{C=N}$ of the pyrazole ring. In all the three complexes the intensity of this band decreases compared to the ligand due to the nitrogen being bonded to the metal center. The little difference in the d–d band for complexes **1** (631 nm) and **3** (624 nm) shows that the coordination sphere should be very similar. Indeed the structural data show that all the complexes **1–3** have N_4O_2 donors and very similar geometry even in terms of the distorted Jahn–Teller axes (Table 1). The structural data for complexes **1–3** show that axial Cu–O bonds [*ca.* 2.31 (4) Å] are relatively longer. There appears to be a red shift for the d–d band of complex **2** since it appears at 641 nm although the coordination environment is similar. This might be due to the change in solvent from acetonitrile to methanol since **2** is not soluble in acetonitrile.

The axial coordination made by the carbonyl oxygen atoms of the amide in bispyrazole based ligand is reported to be relatively labile in solution.[60] Hence the longer Cu–O bonds may be susceptible to dissociation during the redox reaction in presence of H_2A and O_2 and promote the binding of oxygen to the Cu^{II} centre. However the change in coordination environment due to opening of such bonds may lead to instability and possible decomposition during such redox reactions. This becomes evident from the cyclic voltammetry data of the complexes **1–3**. All the three complexes show that a chemical reaction is coupled with the redox processes. This may be because of an unfavourable geometry rendered by the ligand upon reduction by the electrochemical process. Complex **2** shows a redox event at $E_{1/2}$ = −0.097 V (ΔE_p = 193 mV) which may correspond to Cu^{II}/Cu^{I} couple and later another reduction at −0.78 V which might be due to decomposition of Cu^{I} to Cu^{0}. **1** and **3** on the other hand shows a reduction with a maxima at *ca.*

Table 3 Cytotoxic activities of the ligands and complexes **1–3** from three experimental trials with comparison to two well known platinum drugs

IC_{50} (μM) ± S.D.[a]							
	L1	**L2**	**1**	**2**	**3**	Cisplatin	Carboplatin[b]
MCF-7	>250	>250	160 ± 5	116 ± 3	70 ± 2	12 ± 2	62.19

[a] S.D. = standard deviation; IC_{50} values were calculated by variable slope model using Graph pad prism 5.0®. 6×10^3 cells per well were treated for 48 h with increasing concentrations of tested compounds. Cytotoxicity was assessed by MTT test. [b] On drug exposure of 72 h (data taken from ref. 63).

−0.4 V followed by a possible decomposition rendering to Cu^0 at *ca.* −0.74 V for **1** and −0.67 for **2** respectively. The oxidation peak height is significantly shorter that the reduction peak height. The cyclic voltammetry studies suggest that the electrochemical reduction process is coupled with chemical events leading to decomposition and hence irreversibility. The irreversible oxidation peak at 0.62 V only exhibited by complex **2** may be attributed to the oxidation of the chloride anion.

The complexes **1–3** bind to DNA with binding constants (K_b) of the order of 10^4 M^{-1}. The binding constant and the small changes in CT-DNA melting point (Table 2) upon interaction with the complexes signify non-intercalative binding mode and weak interaction. The ligands used are non-planar and hence the interaction observed may be more of electrostatic nature. However, the chemical redox process in presence of H_2A and O_2 lead to complete relaxation of the supercoiled form of pUC19 DNA at a concentration of 100 μM (Fig. 7).

In case of oxidative cleavage, where an external reducing agent is involved along with molecular oxygen, very few time dependent cleavage studies are performed to find out the rate constant since there are multiple dependence factors.[14] However an estimate of the minimum incubation time needed can at least be derived from such studies. Hence, we probed the time dependent DNA cleavage of complexes **1–3** (Fig. 8) and found that they relax SC DNA to its NC form by around 30–60 min. However, the reaction did not appear to be first order with respect to the incubation time. It should be noted that the concentration of H_2A used is five time as compared to the concentration of the complex. The use of a higher amount of H_2A might be needed to get a better correlation of the time dependence with respect to a constant complex concentration, but higher concentration of H_2A also leads to DNA cleavage by itself and hence using a higher concentration of H_2A would be inappropriate for finding out the effect of the complex.

The relaxation of the SC DNA to the NC form by complexes **1–3** at 100 μM concentration is however, not unusual to observe in case of Cu^{II} complexes at such concentrations but the mechanistic studies proved to be interesting. Investigation regarding the ROS species involved in relaxation of SC DNA showed that for **1** and **2** hydroxyl radical and singlet oxygen are not involved as the ROS. Complex **3** showed a significant decrease in the chemical nuclease activity with NaN_3 and especially with histidine which demonstrates that the presence of methionine pendant group involves singlet oxygen as one of the reactive species for DNA cleavage (Fig. 10).

Catalase and 4-carboxy TEMPO radical inhibited DNA cleavage significantly in **1–3** (Fig. 11). These results show that although for **1** and **2** the DNA cleavage is mediated by peroxide only but complex **3** exhibits both peroxide and singlet oxygen based relaxation of SC DNA to its nicked circular form. Complexes **1–3** have almost identical bond parameters for the metal co-ordination sphere (Table 1) and only differ in terms of ethylenediamine and **3** a methionine ester moiety.

The DNA cleavage activity of all the three complexes decreased to 1/3 of its original value (Fig. 11) in presence of catalase which suggests peroxide to be the most active species

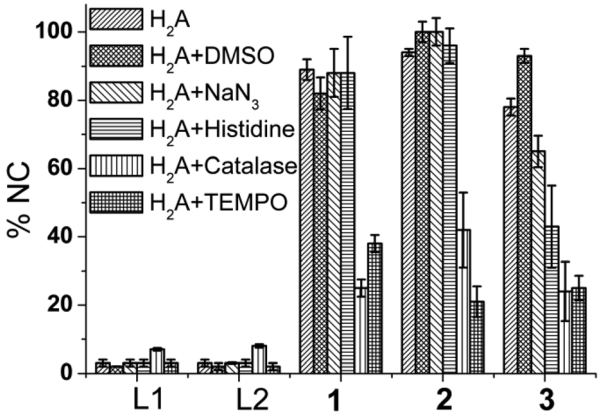

Fig. 11 A typical bar diagram showing the formation of NC form of pUC19 by **L1**, **L2** (100 μM), **1–3** (100 μM) in presence of H_2A and the mechanistic studies with different ROS scavengers for complexes **1–3** (error bars represent standard deviation in data) showing peroxide as the possible ROS.

in DNA cleavage. In addition it should be noted here that although there is an additional pathway active in the methionine complex, the dose response on the DNA cleavage activity is the same in all the three complexes. The above result emphasizes that in case of complex **3** the presence of methionine may promote the otherwise kinetically inhibited reaction of generation of singlet oxygen ($^1O_2$) from peroxide, formed by the Cu^{II} in the complex upon reaction with oxygen in dark.

Complex **3** also shows higher activity in relaxing SC DNA in presence of H_2O_2 compared to **1** or **2** (Fig. S4†). The higher activity of H_2O_2 dependent DNA cleavage in **3** may be because the presence of methionine stabilizes better the Cu–ROS intermediate as compared to **1** and **2**. In presence of H_2O_2 the relaxation activity of supercoiled pUC19 DNA follows the order **3** > **2** > **1** (Fig. S4†). Complex **3** shows *ca.* 72% cleavage at 170 μM concentration whereas complex **1** and **2** shows *ca.* 33 and 40% respectively.

A UV light mediated DNA cleavage was attempted since we found that complex **3** promotes DNA cleavage through singlet oxygen. We found that irradiation with a 4 W 365 nm UV lamp for 30 min followed by an incubation at 37 °C for 1 h in dark did not show any relaxation of SC-DNA in presence of upto 170 μM of **1–3** (Fig. S7†). The presence of 365 nm UV light in combination with the reducing agent H_2A also did not show any improvement over the dark cytotoxicity for **1–3** (Fig. S7†). So the relaxation of supercoiled DNA is clearly mediated through a chemical pathway involving the reducing agent (H_2A) rather than a photochemical pathway.

The complexes showed good correlation between their DNA cleavage and *in vitro* cellular cytotoxicity data. When tested on MCF-7 complex **3** was found to be the most cytotoxic one among the three complexes. We see that although complex **1** is the least hydrophilic (Fig. 6) and hence should be able to better penetrate the cell membrane and accumulate more in cells yet it is the least active one. We find that **2** having the more physiology relevant chloride ion is more active than **1** (Table 3) which might be due to better solubility of complex **2**

as compared to **1**. However, complex **3** is the most active one ($IC_{50} \sim 70$ μM) although least lipophilic suggesting that lipophilicity is a good guideline but the cell might uptake complex **3** more through certain receptors due to the presence of methionine which is one of the essential amino acids and very much needed in cellular metabolism[61,62] and its presence in **3** renders a dual pathway of DNA damage.

Conclusions

Complexes **1–3** show significant DNA cleavage activity at 100 μm concentration and the DNA cleavage in **1** and **2** is mediated through peroxide pathway whereas in **3** both peroxide and singlet oxygen based pathway is active. The DNA cleavage studies emphasize that in Cu^{II} complexes the presence of methionine as a pendant moiety in the ligand can help to generate additional ROS and induce DNA damage through multiple pathways. The results show that methionine based Cu^{II} complexes can generate singlet oxygen even in dark in presence of cellular reducing agents like H_2A. The use of H_2O_2 as activator for **1–3** shows that the presence of methionine also facilitates generation of ROS from H_2O_2 by the Cu^{II} center leading to better relaxation of SC DNA to its NC form. Earlier it was shown that in dark Cu^{II} complexes bearing methionine as part of the ligand shows either hydroxyl radical or singlet oxygen based DNA cleavage activity.[23,27] In this work we confirm that when methionine is present as part of the ligand in Cu^{II} complexes but does not take part in coordination then it can convert a part of the metal generated peroxide to singlet oxygen and activate a dual pathway for relaxing SC DNA, to its nicked circular form. The *in vitro* toxicity data of complex **3** in MCF-7 cancer cell line shows that it is not as toxic ($IC_{50} \sim 70$ μM) as cisplatin ($IC_{50} \sim 12.5$ μM) rather the toxicity is comparable to carboplatin ($IC_{50} \sim 62.5$ μM)[63] or certain gallium based drugs in clinic used to treat various resistant cancers.[64] Improving the design of the methionine conjugated coordinating ligand to better stabilize the $Cu^{I/II}$ state may enhance the anti-cancer activity of such complexes. Hence complex **3** warrants more investigation with this family of ligands keeping the methionine intact but changing the metal and donor sites.

Acknowledgements

We sincerely thank DST for the funding (Vide Project no-SR/S1/IC-36/2010). We are also thankful to IISER Kolkata for the financial and infrastructural support including NMR and single crystal X-ray facilities. SB, SKD and GPJ thank CSIR-India for providing research fellowship. AS sincerely thanks IISER Kolkata for research fellowship.

References

1 O. Arrigoni and M. C. De Tullio, *Biochim. Biophys. Acta, Gen. Subj.*, 2002, **1569**, 1–9.
2 C. L. Linster and E. Van Schaftingen, *FEBS J.*, 2007, **274**, 1–22.
3 D. Zhou, H. Xiao, F. Meng, S. Zhou, J. Guo, X. Li, X. Jing and Y. Huang, *Bioconjugate Chem.*, 2012, **23**, 2335–2343.
4 J. Du, J. J. Cullen and G. R. Buettner, *Biochim. Biophys. Acta, Rev. Cancer*, 2012, **1826**, 443–457.
5 C. Bartel, A. E. Egger, M. A. Jakupec, P. Heffeter, M. Galanski, W. Berger and B. K. Keppler, *J. Biol. Inorg. Chem.*, 2011, **16**, 1205–1215.
6 A. R. Chakravarty and M. Roy, *Prog. Inorg. Chem.*, 2012, **57**, 119–202.
7 M. P. Cervantes-Cervantes, J. V. Calderon-Salinas, A. Albores and J. L. Munoz-Sanchez, *Biol. Trace Elem. Res.*, 2005, **103**, 229–248.
8 D.-D. Li, J.-L. Tian, W. Gu, X. Liu, H.-H. Zeng and S.-P. Yan, *J. Inorg. Biochem.*, 2011, **105**, 894–901.
9 A. Kellett, M. O'Connor, M. McCann, O. Howe, A. Casey, P. McCarron, K. Kavanagh, M. McNamara, S. Kennedy, D. D. May, P. S. Skell, D. O'Shea and M. Devereux, *MedChemComm*, 2011, **2**, 579–584.
10 T. K. Goswami, B. V. S. K. Chakravarthi, M. Roy, A. A. Karande and A. R. Chakravarty, *Inorg. Chem.*, 2011, **50**, 8452–8464.
11 A. K. Patra, T. Bhowmick, S. Roy, S. Ramakumar and A. R. Chakravarty, *Inorg. Chem.*, 2009, **48**, 2932–2943.
12 S. Anbu, M. Kandaswamy, P. Suthakaran, V. Murugan and B. Varghese, *J. Inorg. Biochem.*, 2009, **103**, 401–410.
13 P. U. Maheswari, M. van der Ster, S. Smulders, S. Barends, G. P. van Wezel, C. Massera, S. Roy, H. den Dulk, P. Gamez and J. Reedijk, *Inorg. Chem.*, 2008, **47**, 3719–3727.
14 Y. Jin and J. A. Cowan, *J. Am. Chem. Soc.*, 2005, **127**, 8408–8415.
15 S. Dhar, M. Nethaji and A. R. Chakravarty, *Inorg. Chem.*, 2005, **44**, 8876–8883.
16 S. Borah, M. S. Melvin, N. Lindquist and R. A. Manderville, *J. Am. Chem. Soc.*, 1998, **120**, 4557–4562.
17 M. Subramanian, U. Shadakshari and S. Chattopadhyay, *Bioorg. Med. Chem.*, 2004, **12**, 1231–1237.
18 N. Yamashita, M. Murata, S. Inoue, M. J. Burkitt, L. Milne and S. Kawanishi, *Chem. Res. Toxicol.*, 1998, **11**, 855–862.
19 A. K. Patra, T. Bhowmick, S. Ramakumar, M. Nethaji and A. R. Chakravarty, *Dalton Trans.*, 2008, 6966–6976.
20 B. Macias, M. V. Villa, B. Gomez, J. Borras, G. Alzuet, M. Gonzalez-Alvarez and A. Castineiras, *J. Inorg. Biochem.*, 2007, **101**, 444–451.
21 F. Arjmand, M. Muddassir and R. H. Khan, *Eur. J. Med. Chem.*, 2010, **45**, 3549–3557.
22 Y. Huang, Q.-S. Lu, J. Zhang, Z.-W. Zhang, Y. Zhang, S.-Y. Chen, K. Li, X.-Y. Tan, H.-H. Lin and X.-Q. Yu, *Bioorg. Med. Chem.*, 2008, **16**, 1103–1110.
23 C. Gao, X. Ma, J. Lu, Z. Wang, J. Tian and S. Yan, *J. Coord. Chem.*, 2011, **64**, 2157–2169.
24 H. Ahsan and S. M. Hadi, *Cancer Lett.*, 1998, **124**, 23–30.
25 K. Satoh, T. Kadofuku and H. Sakagami, *Anticancer Res.*, 1997, **17**, 2487–2490.

26 H. Sakagami, K. Satoh, T. Kadofuku and M. Takeda, *Anticancer Res.*, 1997, **17**, 2565–2570.
27 A. K. Patra, S. Dhar, M. Nethaji and A. R. Chakravarty, *Dalton Trans.*, 2005, 896–902.
28 A. K. Patra, S. Dhar, M. Nethaji and A. R. Chakravarty, *Chem. Commun.*, 2003, 1562–1563.
29 P. K. Sasmal, A. K. Patra, M. Nethaji and A. R. Chakravarty, *Inorg. Chem.*, 2007, **46**, 11112–11121.
30 T. K. Goswami, M. Roy, M. Nethaji and A. R. Chakravarty, *Organometallics*, 2009, **28**, 1992–1994.
31 T. K. Goswami, S. Gadadhar, M. Roy, M. Nethaji, A. A. Karande and A. R. Chakravarty, *Organometallics*, 2012, **31**, 3010–3021.
32 M. A. Pereira, W. Wang, P. M. Kramer and L. Tao, *Toxicol. Sci.*, 2004, **77**, 243–248.
33 J. M. Mato, M. L. Martinez-Chantar and S. C. Lu, *Amino Acids in Hum. Nutr. Health*, 2012, 173–188.
34 P. D. King and M. C. Perry, *Oncologist*, 2001, **6**, 162–176.
35 H. J. Zimmerman, *Hepatotoxicity: The Adverse Effects of Drugs and Other Chemicals on the Liver*, 1978.
36 H. J. Zimmerman and W. C. Maddrey, *Hepatology*, 1995, **22**, 767–773.
37 A. T. Banks, H. J. Zimmerman, K. G. Ishak and J. G. Harter, *Hepatology*, 1995, **22**, 820–827.
38 H. J. Zimmerman, *Liver: Norm. Funct. Dis.*, 1980, **2**, 687–737.
39 D. D. Perrin and W. L. F. Armarego, *Purification of Laboratory Chemicals*, 3rd edn, 1988.
40 N. Burzlaff, I. Hegelmann and B. Weibert, *J. Organomet. Chem.*, 2001, **626**, 16–23.
41 C. D. Vo, D. Kuckling, H. J. P. Adler and M. Schonhoff, *Colloid Polym. Sci.*, 2002, **280**, 400–409.
42 C. Dubuisson, Y. Fukumoto and L. S. Hegedus, *J. Am. Chem. Soc.*, 1995, **117**, 3697–3704.
43 G. M. Sheldrick, *Z. Kristallogr.*, 2002, **217**, 644–650.
44 G. M. Sheldrick, *Int. Union Crystallogr., Crystallogr. Symp.*, 1991, **5**, 145–157.
45 P. Van der Sluis and A. L. Spek, *Acta Crystallogr., Sect. A: Fundam. Crystallogr.*, 1990, **46**, 194–201.
46 M. E. Reichmann, C. A. Rice, C. A. Thomas and P. Doty, *J. Am. Chem. Soc.*, 1954, **76**, 3047–3053.
47 J. Marmur, *J. Mol. Biol.*, 1961, **3**, 208–218.
48 B. Macias, I. Garcia, M. V. Villa, J. Borras, M. Gonzalez-Alvarez and A. Castineiras, *J. Inorg. Biochem.*, 2003, **96**, 367–374.
49 J. Hong, Y. Jiao, J. Yan, W. He, Z. Guo, L. Zhu and J. Zhang, *Inorg. Chim. Acta*, 2010, **363**, 793–798.
50 C. A. Detmer III, F. V. Pamatong and J. R. Bocarsly, *Inorg. Chem.*, 1996, **35**, 6292–6298.
51 M. Gonzalez-Alvarez, G. Alzuet, J. Borras, B. Macias and A. Castineiras, *Inorg. Chem.*, 2003, **42**, 2992–2998.
52 C. Zhang, Y. Wang and F. Wang, *Bull. Korean Chem. Soc.*, 2007, **28**, 1183–1186.
53 J. Sangster and A. D. Pelton, *J. Phys. Chem. Ref. Data*, 1987, **16**, 509–561.
54 T. Mosmann, *J. Immunol. Methods*, 1983, **65**, 55–63.
55 B. L. Lokeshwar, E. Escatel and B. Zhu, *Curr. Med. Chem.*, 2001, **8**, 271–279.
56 M. C. Alley, D. A. Scudiero, A. Monks, M. L. Hursey, M. J. Czerwinski, D. L. Fine, B. J. Abbott, J. G. Mayo, R. H. Shoemaker and M. R. Boyd, *Cancer Res.*, 1988, **48**, 589–601.
57 N. E. Brese and M. O'Keeffe, *Acta Crystallogr., Sect. B: Struct. Sci.*, 1991, **47**, 192–197.
58 A. Wolfe, G. H. Shimer Jr. and T. Meehan, *Biochemistry*, 1987, **26**, 6392–6396.
59 W. M. Tay, J. D. Epperson, G. F. Z. da Silva and L.-J. Ming, *J. Am. Chem. Soc.*, 2010, **132**, 5652–5661.
60 M. Giorgetti, S. Tonelli, A. Zanelli, G. Aquilanti, M. Pellei and C. Santini, *Polyhedron*, 2012, **48**, 174–180.
61 F. Hirche, A. Schroeder, B. Knoth, G. I. Stangl and K. Eder, *Br. J. Nutr.*, 2006, **95**, 879–888.
62 R. L. Levine, J. Moskovitz and E. R. Stadtman, *IUBMB Life*, 2000, **50**, 301–307.
63 Y.-E. Kwon, J.-Y. Park and W.-K. Kim, *Anticancer Res.*, 2007, **27**, 321–326.
64 L. R. Bernstein, in *Metallotherapeutic Drugs and Metal-Based Diagnostic Agents*, John Wiley & Sons, Ltd, 2005, pp. 259–277.